ECCOMAS Thematic Conference on Mechanical Response of Composites
P.P. Camanho et.al. (eds.)
Porto, Portugal, 12–14 September 2007

NONLINEAR CONSTITUTIVE FORMULATION FOR A FINITE DEFORMATION BEAM MODEL BASED ON THE MIXING RULE FOR COMPOSITES

P. Mata A.[1], S. Oller[1], A.H. Barbat[1] and R. Boroschek K[2]

[1]Technical University of Catalonia
Edifici C1, Campus Nord UPC Gran Capità s/n 08034. Barcelona, Spain.
e-mail: pmata@cimne.upc.edu, sergio.oller@upc.edu, alex.barbat@upc.edu

[2]University of Chile, Civil Engineering Department
Blanco Encalada 2002. Santiago, Chile.
e-mail: rborosch@ing.uchile.cl

Keywords: Geometric nonlinearity, nonlinear analysis, beam model, composites, reinforced concrete structures, damage index, mixing theory.

Abstract. *Constitutive nonlinearity for beam models has been traditionally described by means of concentrated and distributed models, in the most cases, formulated assuming infinitesimal deformation. The concentrated models consider elastic elements equipped with plastic hinges at the ends. In the case of distributed plasticity models, inelasticity is evaluated at a fixed number of points on the cross sections and along the beam axis. These points corresponds to of fibers directed along the axis. Therefore, this approach is referred as fiber approach. Additionally, two versions of the models can be defined: the displacement based method, which is based on the interpolation of the strain field along the elements and force based method which obtains the sectional forces and moments interpolating the nodal values and satisfying the equilibrium equations even in the inelastic range. Both approaches are affected by the strain localization phenomenon when materials with softening behavior are employed and, therefore, the whole structural response becomes mesh dependent if no appropriate corrections are considered. On the another hand, one of the most invoked geometrically exact formulations for beams in finite deformation is that of Simo which generalize to the 3–D dynamic case the formulation developed by Reissner. Only a few works have developed fully geometrical and constitutive nonlinear formulations for beams, but they have been mainly focused on plasticity. Recently, Mata et.al. [14, 15] have extended the formulation due to Reissner-Simo for considering and arbitrary distribution of composite materials on the cross sections for the static and dynamic cases. The displacement based method is used for solving the resulting nonlinear problem. Thermodynamically consistent constitutive laws are used in describing the material behavior of simple materials and the parallel version of the mixing rule is used for composites. In this work a detailed presentation of the implementation of the mixing rule for the treatment of constitutive nonlinearity in the Reissner–Simo formulation for beams is presented. Finally, several numerical examples validating the proposed formulation are given.*

1 INTRODUCTION

The three dimensional nonlinear analysis of beam structures has captured the interest of many researchers during the past decades. As mentioned by Nukala *et.al.* [19], many contributions have been focused on the formulation of geometrically consistent models of beams undergoing large displacements and rotations, but considering that the material behavior remains elastic. On the contrary, the constitutive nonlinearity in beams has been described by means of *concentrated* and *distributed* models, both of them formulated for small strain and small displacement kinematic hypothesis. Only a few works have been carried out using a fully geometrical and material nonlinear formulations for beams, but they have been mainly focused on plasticity.

One of the most invoked geometrically exact formulations is that of Simo [23], which generalize to the 3D case the formulation originally developed by Reissner [20] for the plane static problem. Posteriorly, Simo and Vu-Quoc [24, 25] implemented the numerical integration of the equations of motion of rods in the context of the finite element (FE) framework for the static and dynamic cases. Ibrahimbegović to extend the formulation given in reference [23] to the case of a curved reference configuration of the rod [7]. A formulation equivalent to that proposed by Simo has been employed by Cardona and Huespe [2] for evaluating the bifurcation points along the nonlinear equilibrium trajectory of flexible mechanisms and by Ibrahimbegović *et.al.* in [8] for studying the buckling and post buckling behavior of framed structures.

Works on constitutive nonlinearity have progressed based on a different approach, that's, *lumped* and *distributed* plasticity models. The lumped plasticity models consider linear elastic structural elements equipped with plastic hinges at the ends. But it is important to note that the nonlinear constitutive laws are valid only for specific geometries of the beam cross section [6]. In the case of distributed models, the constitutive nonlinearity is evaluated at a fixed number of cross sections along the beam axis, allowing to obtain a distributed nonlinear behavior along the structural elements. These sections are divided into a number of control points corresponding to fibers directed along the beam's axis. Therefore, this approach is frequently referred as *fiber approach*.

Usually, beam models are affected by the strain localization phenomenon when materials with softening behavior are employed. In any case, the whole structural response becomes mesh dependent if no appropriate corrections are considered. Several techniques have been proposed for ensuring objectivity of the structural element response. For example, Hanganu *et.al.* [6] and Barbat *et.al.* [1] regularize the energy dissipated at material point level, limiting its value to the specific fracture energy of the material. One of the most common limitations of the distributed formulations lies in the fact that inelasticity is defined for the component of the strain acting in the direction normal to the face of the cross section and, therefore, the shearing components of the stress are treated elastically [4].

Works considering both constitutive and geometric nonlinearity are scarce and they have been mainly restricted to plasticity [14, 15, 21]. Outstanding works considering warping of arbitrary sections made of rate dependent and rate independent elastic–plastic material are proposed by Simo *et.al.* [26] and Gruttmann *et.al.* [5] respectively, while Kumar and White [19] develop a mixed finite element for studying the stability of steel structures.

In this work, the general nonlinear constitutive behavior is included in the static version of the geometrically exact formulation for beams proposed by Simo, considering a curved reference configuration. The displacement based method is used for solving the resulting nonlinear problem. Plane cross sections remain plane after the deformation of the structure; therefore, no

cross sectional warping is considered. An appropriated cross sectional analysis is applied for obtaining the cross sectional forces and moments and the consistent tangential tensors in the linearized problem. Thermodynamically consistent constitutive laws are used in describing the material behavior and the simple mixing rule is also considered in modeling materials which are composed by several components. Special attention is paid to the obtention of a structural damage indices.

2 FINITE STRAIN FORMULATION FOR INITIALLY CURVED BEAMS

The formulation of Simo and Vu Quoc [23, 24] for beams that can undergo large deformations in space is expanded considering an intermediate curved reference configuration [7]. The description of both the geometry and the kinematics of the beam is developed in the nonlinear differential manifold $\mathbb{R}^3 \times SO(3)$, where the rotation manifold is denoted by $SO(3)$ [24].
Let $\{\hat{E}_i\}$ and $\{\hat{e}_i\}$ $(i = 1 \dots 3)$ be the spatially fixed *material* and *spatial* frames, respectively. The straight reference beam is defined by $\hat{\varphi}_{00} = S\hat{E}_1$, with $S \in [0, L] \subset \mathbb{R}$ its arch–length coordinate. Beam cross sections are described by means of the coordinates ξ_β directed along $\{\hat{E}_{\beta=2,3}\}$ and, therefore, the position vector of any material point is $\hat{X} = S\hat{E}_1 + \xi_\beta \hat{E}_\beta$.
The curved reference beam is defined by means of a fixed curve with position vector given by $\hat{\varphi}_0 = \varphi_{0i}(S)\hat{e}_i \in \mathbb{R}^3$. Additionally, each point on this curve has rigidly attached an orthogonal local frame $\hat{t}_{0i}(S) = \mathbf{\Lambda}_0 \hat{E}_i \in \mathbb{R}^3$, where $\mathbf{\Lambda}_0 \in SO(3)$ is the orientation tensor. The beam cross section $\mathcal{A}(S)$ is defined considering the local coordinate system ξ_β but directed along $\{\hat{t}_{0\beta}\}$. The planes of the cross sections are normal to the vector tangent to the reference curve, *i.e.* , $\hat{\varphi}_{0,S} = \hat{t}_{01}$. The position vector of any material point on the curved reference beam is $\hat{x}_0 = \hat{\varphi}_0 + \mathbf{\Lambda}_0 \xi_\beta \hat{E}_\beta \in \mathcal{A}(S) \times [0, L]$.
The motion deforms $\hat{\varphi}_0(S)$ to $\hat{\varphi}(S, t)$ at time t, adding a translational displacement $\hat{u}$, *i.e.* $\hat{\varphi} = \hat{\varphi}_0 + \hat{u}$. The local orientation frame is simultaneously rotated from $\mathbf{\Lambda}_0(S)$ to $\mathbf{\Lambda}(S, t)$ by means of the *incremental rotation tensor* $\mathbf{\Lambda}_n(S, t)$ [23, 24], *i.e.* , $\mathbf{\Lambda} = \mathbf{\Lambda}_n \mathbf{\Lambda}_0$ (see Figure 1).

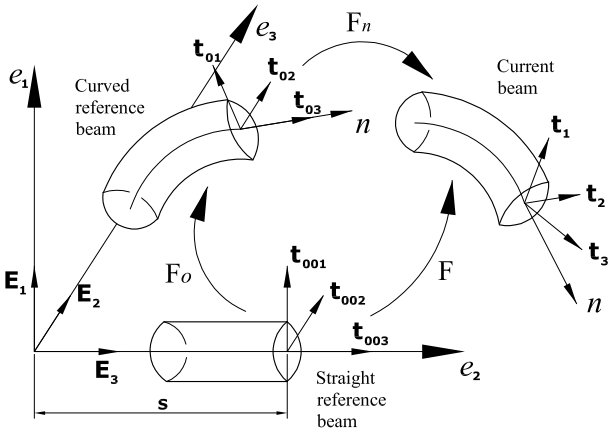

Figure 1: Configurational description of the beam.

In general, the normal vector $\hat{t}_1 \neq \hat{\varphi}_{,S}$ because of the shearing. The position vector of any material point on the current beam is given by

$$\hat{x}(S, \xi_1, \xi_2, t) = \hat{\varphi}(S, t) + \xi_\beta \hat{t}_\beta(S, t) = \hat{\varphi} + \mathbf{\Lambda} \xi_\beta \hat{E}_\beta \tag{1}$$

Eq. (1) implies that the current beam configuration is completely determined by the pairs $(\hat{\varphi}, \mathbf{\Lambda}) \in \mathbb{R}^3 \times SO(3)$ [12, 24] and the *spatial placement of the beam* is defined as

$$\mathcal{B}_t := \{\hat{x} \in \mathbb{R}^3 \,\big|\, \hat{\varphi}_0 + \mathbf{\Lambda}\xi_\beta \hat{E}_\beta;\ \ (S, \xi_\beta) \in [0, L] \times \mathcal{A}\} \tag{2}$$

The *tangent space* to $\mathcal{B}_t$ at $\hat{x}$ is given by $T_{\hat{x}}\mathcal{B}_t := \{\delta\hat{x} \in \mathbb{R}^3 \,|\, \hat{x} \in \mathcal{B}_t\}$ for any variation $\delta\hat{x}$ obtained from the kinematically admissible variation of the variables defining current configuration *i.e.* $(\delta\hat{\varphi}, \delta\hat{\theta}) \in \mathbb{R}^3 \times T^{\text{spa}}_{\mathbf{\Lambda}}$, so that $\delta\mathbf{\Lambda} = (\delta\hat{\theta} \times \mathbf{\Lambda}) \in T^{\text{spa}}_{\mathbf{\Lambda}} SO(3)$ [12][1]. Fixing the time $t = t_0$ or $t = t_{00}$, it is possible to define the initial placement $\mathcal{B}_0$ and its tangent space $T_{\hat{X}}\mathcal{B}_0$ for the curved reference beam and $\mathcal{B}_{00}$ and $T_{\hat{X}}\mathcal{B}_{00}$ for the straight reference beam.
The deformation gradients of the curved reference beam and of the current beam referred to the straight reference configuration are denoted by $\mathbf{F}_0$ and $\mathbf{F}$, respectively. Explicit expressions for them are [9]

$$\mathbf{F}_0 = [\widetilde{\boldsymbol{\omega}}_0 \xi_\beta \hat{t}_{0\beta}] \otimes \hat{E}_1 + \mathbf{\Lambda}_0, \qquad \mathbf{F} = [\hat{\varphi}_{,S} - \hat{t}_1 + \widetilde{\boldsymbol{\omega}} \xi_\beta \hat{t}_\beta] \otimes \hat{E}_1 + \mathbf{\Lambda} \tag{3}$$

where $\widetilde{\boldsymbol{\omega}}_0 \equiv \mathbf{\Lambda}_{0,S}\, \mathbf{\Lambda}_0^T \in T^{\text{spa}}_{\mathbf{\Lambda}} SO(3) \approx so(3)$ is the curvature tensor of the curved reference beam referred to the straight beam. It is worth noting that in Eq. (3) the term defined as $\hat{\gamma} = \hat{\varphi}_{,S} - \hat{t}_1$ corresponds to the reduced strain measure of shearing and elongation [9, 23] which, in conjunction with the curvature tensor $\widetilde{\boldsymbol{\omega}} \equiv \mathbf{\Lambda}_{,S}\, \mathbf{\Lambda}^T \in so(3)$, allows measuring the strain state $\hat{\varepsilon}$ existing in each material point of the current beam cross section referred to the straight reference beam, *i.e.* $\hat{\varepsilon} = \hat{\gamma} + \widetilde{\boldsymbol{\omega}} \xi_\beta \hat{t}_\beta$ The deformation gradient $\mathbf{F}_n := \mathbf{F}\mathbf{F}_0^{-1} : T_{\hat{X}}\mathcal{B}_0 \to T_{\hat{x}}\mathcal{B}_t$ relating the differential arch length elements of the curved reference configuration with the current placement is responsible for the development of strains, and it can be expressed as [9, **?**]

$$\mathbf{F}_n = \mathbf{F}\mathbf{F}_0^{-1} = |\mathbf{F}_0|^{-1}[\hat{\varphi}_{,S} - \mathbf{\Lambda}_n \hat{\varphi}_{0,S} + \widetilde{\boldsymbol{\omega}}_n \xi_\beta \hat{t}_\beta] \otimes \hat{t}_{01} + \mathbf{\Lambda}_n \tag{4}$$

where $\widetilde{\boldsymbol{\omega}}_n \equiv \mathbf{\Lambda}_{n,S}\, \mathbf{\Lambda}_n^T \in so(3)$ is the current curvature tensor referred to the curved reference beam and $|\mathbf{F}_0|$ is the determinant of $\mathbf{F}_0$. The material representation of $\mathbf{F}_n$ and $\widetilde{\boldsymbol{\omega}}_n$ are obtained as $\mathbf{F}_n^{\text{m}} = \mathbf{\Lambda}^T \mathbf{F}_n \mathbf{\Lambda}_0$ and $\widetilde{\mathbf{\Omega}}_n = \mathbf{\Lambda}^T \widetilde{\boldsymbol{\omega}}_n \mathbf{\Lambda}$. Removing the rigid body component $\mathbf{\Lambda}_n$ from $\mathbf{F}_n$, it is possible to construct the strain tensor $\boldsymbol{\varepsilon}_n = \mathbf{F}_n - \mathbf{\Lambda}_n \in T_{\hat{x}}\mathcal{B}_t \otimes T_{\hat{X}}\mathcal{B}_0$, conjugated to the asymmetric *First Piola Kirchhoff* (FPK) stress tensor $\mathbf{P} = \hat{P}_j \otimes \hat{t}_{0j} \in T_{\hat{x}}\mathcal{B}_t \otimes T_{\hat{X}}\mathcal{B}_0$, which is referred to the curved reference beam [23]. By other hand, the spatial strain vector acting on the current beam cross section relative to an element of area in the curved reference beam is obtained as $\hat{\varepsilon}_n = \boldsymbol{\varepsilon}_n \hat{t}_{01}$.

2.1 Stress vector and cross sectional stress resultants

The strain vector $\hat{\varepsilon}_n$ is energetically conjugated to the asymmetric *First Piola Kirchhoff* (FPK) stress vector [23, 9], which can be defined as $\hat{P}_1 = P_{1j}\hat{t}_j \in T^*_{\hat{x}}\mathcal{B}_t$, where P_{1j} is the component of the stress vector acting on the direction j of the local frame attached to the current cross section relative to the direction $\hat{t}_{0j}$ in the corresponding curved reference configuration. The cross sectional *stress resultant* and the *stress couple* vectors are

$$\hat{n}(S) = \int_{\mathcal{A}} \hat{P}_1 d\mathcal{A} \quad \in T^*_{\hat{x}}\mathcal{B}_t; \qquad \hat{m}(S) = \int_{\mathcal{A}} (\hat{x} - \hat{\varphi}) \times \hat{P}_1 d\mathcal{A} \quad \in T^*_{\hat{x}}\mathcal{B}_t \tag{5}$$

The corresponding material descriptions are $\hat{n}^{\text{m}} = \mathbf{\Lambda}^T \hat{n}$, $\hat{m}^{\text{m}} = \mathbf{\Lambda}^T \hat{m}$ and $\hat{P}_1^{\text{m}} = \mathbf{\Lambda}^T \hat{P}_1$.

[1]The symbol $T^{\text{spa}}_{\mathbf{\Lambda}} SO(3)$ denotes the spatial form of the tangential space to SO(3), with base point $\mathbf{\Lambda}$, and $T^{\text{spa}}_{\mathbf{\Lambda}}$ is the spatial linear vector space of rotations, with base point $\mathbf{\Lambda}$, as described in Ref. [12].

2.2 Virtual work principle

The spatial form of the *reduced balance equations* of the current beam, referred to the curved reference beam, can be written as [9]

$$\hat{n}_{,S} + \hat{n}_p = 0; \qquad \hat{m}_{,S} + \hat{\varphi}_{,S} \times \hat{n} + \hat{m}_p = 0 \tag{6}$$

where $\hat{n}_p$ and $\hat{m}_p$ are the time varying external *body force* and *body moment* per unit of reference length, respectively. Considering a kinematically admissible variation $h = (\delta\hat{\varphi}, \delta\hat{\theta}) \in \mathbb{R}^3 \times T^{\text{spa}}_{\mathbf{\Lambda}}$ [24], taking the dot product of h with Eqs. (6), integrating over the length of the curved reference beam and integrating by parts for the terms $\hat{n}_{,S}$ and $\hat{m}_{,S}$, one may obtain the following nonlinear functional, $\mathbf{G}(\hat{\varphi}, \mathbf{\Lambda}, h)$, corresponding to the spatial description of the *virtual work principle*:

$$\begin{aligned} \mathbf{G}(\hat{\varphi}, \mathbf{\Lambda}, h) \;=\; & \underbrace{\int_L \Big[(\delta\hat{\varphi}_{,S} - \delta\hat{\theta} \times \hat{\varphi}_{,S}) \cdot \hat{n} + \delta\hat{\theta}_{,S} \cdot \hat{m} \Big] \mathrm{d}S}_{\mathbf{G}_{\text{int}}(\hat{\varphi}, \mathbf{\Lambda}, h)} \\ - \; & \underbrace{\int_L \Big[\delta\hat{\varphi} \cdot \hat{n}_p + \delta\hat{\theta} \cdot \hat{m}_p \Big] \mathrm{d}S}_{\mathbf{G}_{\text{ext}}(\hat{\varphi}, \mathbf{\Lambda}, h)} - \Big[(\delta\hat{\varphi} \cdot \hat{n}) \Big|_0^L + (\delta\hat{\theta} \cdot \hat{m}) \Big|_0^L \Big] = 0 \end{aligned} \tag{7}$$

The functional $\mathbf{G}$ corresponds to the weak form of the balance equations [7, 24]. Noting that $\mathbf{\Lambda}_0$ is a fixed frame, we have that $\delta\hat{\theta} = \delta\hat{\theta}_n$ and, therefore, the terms $(\delta\hat{\varphi}_{,S} - \delta\hat{\theta} \times \hat{\varphi}_{,S})$ and $\delta\hat{\theta}_{,S}$ correspond to the co–rotated variations of the reduced strain measures $\hat{\varepsilon}_n$ and $\hat{\omega}_n$ relative to the curved reference beam, $\delta\, \overset{\triangledown}{[\hat{\gamma}_n]}$ and $\delta\, \overset{\triangledown}{[\hat{\omega}_n]}$, respectively.

3 NONLINEAR CONSTITUTIVE MODELS

In this work, material points on the beam cross sections are considered as formed by a *composite material* corresponding to a homogeneous mixture of different simple *components*, each of them with its own constitutive law (see Figure 2). The behavior of the composite is obtained by means of the *mixing theory* described in following sections.

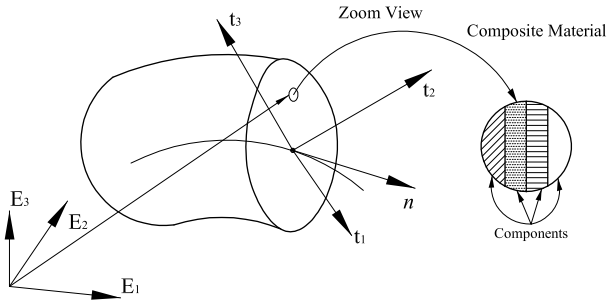

Figure 2: Cross section showing the composite associated to a material point on the current configuration.

3.1 Simple components

Two kinds of nonlinear constitutive models for simple components are used in this work: the *damage* and *plasticity* models. They have been chosen due to the fact that combining different mechanical parameters and using the parallel version of the *mixing rule* for composites [17], a

wide variety of mechanical behaviors can be reproduced. The constitutive models are formulated in terms of the material form of the FPK stress and strain vectors, $\hat{P}_1^{\mathrm{m}}$ and $\hat{\mathcal{E}}_n$, respectively. The resulting components of the material form of the stress resultant and stress couple vectors have the same values as their spatial counterparts described in $\{\hat{t}_i\}$.

3.1.1 Degrading materials: damage model

The damage theory employed in this work is based on a special damage yielding function which differentiates the mechanical response for tension or compression components of the stress vector. The progress of the damage is based on the evolution of a scalar parameter which affects all the components of the elastic constitutive tensor and in this sense, it constitutes an isotropic damage model.

Constitutive Equation and mechanical dissipation. In the case of thermally stable problems, this model has associated the following expression for the free energy density Ψ in terms of the elastic free energy density Ψ_0 and the damage internal variable d [13]:

$$\Psi(\hat{\mathcal{E}}_n, d) = (1-d)\Psi_0 = (1-d)(\frac{1}{2\rho_0}\hat{\mathcal{E}}_n \cdot (\boldsymbol{\mathcal{C}}^{\mathrm{me}}\hat{\mathcal{E}}_n)) \tag{8}$$

where $\hat{\mathcal{E}}_n$ is the material form of the strain vector, ρ_0 is the mass density in the curved reference configuration and $\boldsymbol{\mathcal{C}}^{\mathrm{me}} = \mathrm{Diag}[E_0, G_0, G_0]$ is the material form of the *elastic constitutive tensor*, with E_0 and G_0 the Young and shear undamaged elastic modulus. In this case, considering that the *Clausius Planck* (CP) inequality for the *mechanical dissipation* is valid, its local form [10, 13] can be written as

$$\dot{\Xi}_m = \frac{1}{\rho_0}\hat{P}_1^{\mathrm{m}} \cdot \dot{\hat{\mathcal{E}}}_n - \dot{\Psi} = \big(\frac{1}{\rho_0}\hat{P}_1^{\mathrm{m}} - \frac{\partial \Psi}{\partial \hat{\mathcal{E}}_n}\big) \cdot \dot{\hat{\mathcal{E}}}_n - \frac{\partial \Psi}{\partial d}\dot{d} \geq 0 \tag{9}$$

where $\dot{\Xi}_m$ is the dissipation rate. For the unconditional fulfilment of the CP inequality and applying the Coleman's principle, we have that the arbitrary temporal variation of the free variable $\dot{\hat{\mathcal{E}}}_n$ must be null [10]. In this manner, the following constitutive relation for the material form of the FPK stress vector acting on each material point of the beam cross section is obtained:

$$\hat{P}_1^{\mathrm{m}} = (1-d)\boldsymbol{\mathcal{C}}^{\mathrm{me}}\hat{\mathcal{E}}_n = \boldsymbol{\mathcal{C}}^{\mathrm{ms}}\hat{\mathcal{E}}_n = (1-d)\hat{P}_{01}^{\mathrm{m}} \tag{10}$$

where $\boldsymbol{\mathcal{C}}^{\mathrm{ms}} = (1-d)\boldsymbol{\mathcal{C}}^{\mathrm{me}}$ and $\hat{P}_{01}^{\mathrm{m}} = \boldsymbol{\mathcal{C}}^{\mathrm{me}}\hat{\mathcal{E}}_n$ are the material form of the *secant constitutive tensor* and the *elastic* FPK stress vector, respectively.

Damage yield criterion. The damage yield criterion denoted by the scalar value $\mathcal{F}$ is defined as a function of the undamaged elastic free energy density and written in terms of the components of the material form of the undamaged principal stresses [1, 6], $\hat{P}_{p0}^{\mathrm{m}}$, as

$$\mathcal{F} = \mathcal{P} - f_c = [1 + r(n-1)]\sqrt{\sum_{i=1}^{3}(P_{p0i}^{\mathrm{m}})^2} - f_c \leq 0 \tag{11}$$

where $\mathcal{P}$ is the equivalent (scalar) stress and the parameters r and n given in function of the tension and compression strengths f_c and f_t and the parts of the free energy density developed

when the tension or compression limits are reached, $(\Psi_t^0)_L$ and $(\Psi_c^0)_L$, respectively, are defined as

$$(\Psi_{t,c}^0)_L = \sum_{i=1}^{3} \frac{\langle \pm P_{p0i}^{\rm m} \rangle \mathcal{E}_{ni}}{2\rho_0}; \quad \Psi_L^0 = (\Psi_t^0)_L + (\Psi_c^0)_L; \quad f_t = (2\rho \Psi_t^0 E_0)_L^{\frac{1}{2}} \tag{12a}$$

$$f_c = (2\rho \Psi_c^0 E_0)_L^{\frac{1}{2}}; \quad n = \frac{f_c}{f_t}; \quad r = \frac{\sum_{i=1}^{3} \langle P_{p0i}^{\rm m} \rangle}{\sum_{i=1}^{3} |P_{p0i}^{\rm m}|} \tag{12b}$$

where $|u|$ is the absolute value function and $\langle \pm u \rangle = 1/2(|u| \pm u)$ is the McAuley's function, $\forall\, u \in \mathbb{R}$. A more general expression equivalent to that given in Eq. (11) [1] is the following:

$$\bar{\mathcal{F}} = \mathcal{G}(\mathcal{P}) - \mathcal{G}(f_c) \tag{13}$$

where $\mathcal{G}(\mathcal{P})$ is a scalar monotonic function to be defined in such way to ensure that the energy dissipated by the material on an specific integration point is limited to the specific energy fracture of the material.

Evolution of the damage variable. The evolution law for the internal damage variable d is given by

$$\dot{d} = \dot{\mu} \frac{\partial \bar{\mathcal{F}}}{\partial \mathcal{P}} = \dot{\mu} \frac{\partial \mathcal{G}}{\partial \mathcal{P}} \tag{14}$$

where $\dot{\mu} \geq 0$ is the *damage consistency* parameter. A damage yield condition $\bar{\mathcal{F}} = 0$ and consistency condition $\dot{\bar{\mathcal{F}}} = 0$ are defined analogously as in plasticity theory. By one hand, the yield condition implies that

$$\mathcal{P} = f_c; \qquad \frac{\mathrm{d}\mathcal{G}(\mathcal{P})}{\mathrm{d}\mathcal{P}} = \frac{\mathrm{d}\mathcal{G}(f_c)}{\mathrm{d}f_c} \tag{15}$$

and the consistency condition along with an appropriated definition of the damage variable ($d = \mathcal{G}(f_c)$), allows to obtain the following expression for the damage consistency parameter:

$$\dot{\mu} = \dot{\mathcal{P}} = \dot{f}_c = \frac{\partial \mathcal{P}}{\partial \hat{P}_{01}^{\rm m}} \cdot \dot{\hat{P}}_{01}^{\rm m} = \frac{\partial \mathcal{P}}{\partial \hat{P}_{01}^{\rm m}} \cdot \mathcal{C}^{\rm me} \dot{\hat{\mathcal{E}}}_n \tag{16}$$

Details regarding the deduction of Eqs. (15) and (16) can be consulted in references [1, 6]. These results allow to rewrite Eq. (14) as

$$\dot{\Xi}_m = \Psi_0 \Big[\frac{\mathrm{d}\mathcal{G}}{\mathrm{d}\mathcal{P}} \frac{\partial \mathcal{P}}{\partial \hat{P}_{01}^{\rm m}} \Big] \cdot \boldsymbol{\mathcal{C}}^{\rm me} \dot{\hat{\mathcal{E}}}_n; \quad \dot{d} = \frac{\mathrm{d}\mathcal{G}}{\mathrm{d}\mathcal{P}} \dot{\mathcal{P}} \tag{17}$$

Finally, the Kuhn-Thucker relations: (a) $\dot{\mu} \geq 0$ (b) $\bar{\mathcal{F}} \leq 0$ (c) $\dot{\mu} \bar{\mathcal{F}} = 0$, have to be employed to derive the unloading–reloading conditions *i.e.* if $\bar{\mathcal{F}} < 0$ the condition (c) imposes $\dot{\mu} = 0$, on the contrary, if $\dot{\mu} > 0$ then $\mathcal{F} = 0$.

Definition of $\mathcal{G}$. The following expression is employed for the function $\mathcal{G}$ of Eq. (13) [1]

$$\mathcal{G}(\chi) = 1 - \frac{\bar{\mathcal{G}}(\chi)}{\chi} = 1 - \frac{\chi^*}{\chi} e^{\kappa(1 - \frac{\chi}{\chi^*})} \tag{18}$$

where the term $\bar{\mathcal{G}}(\chi)$ gives the initial yield stress for certain value of the scalar parameter $\chi = \chi^*$ and for $\chi \to \infty$ the final strength is zero. The parameter κ of Eq. (18) is calibrated to obtain

an amount of dissipated energy equal to the specific fracture energy of the material when all the deformation path is followed. Integrating Eq. (9) for an uniaxial tension process with a monotonically increasing load, and considering that in this case the elastic free energy density can be written as $\Psi_0 = \mathcal{P}^2/(2n^2E_0)$ [1], it is possible to obtain that the total energy dissipated is

$$\Xi_t^{\max} = \int_{\mathcal{P}^*}^{\infty} \underbrace{\frac{\mathcal{P}^2}{2\rho_0 n^2 E^0}}_{\Psi_0} \mathrm{d}\mathcal{G}(\mathcal{P}) = \frac{\mathcal{P}^{*2}}{2\rho_0 E^0}\big[\frac{1}{2} - \frac{1}{\kappa}\big]. \tag{19}$$

Therefore, the following expression is obtained for κ

$$\kappa = \frac{1}{\frac{\Xi_t^{\max} n^2 \rho_0 E^0}{f_c^2} - \frac{1}{2}} \geq 0 \tag{20}$$

where it has been assumed that the equivalent stress tension $\mathcal{P}^*$ is equal to the initial damage stress f_c. The values of the maximum dissipation in tension $\Xi_t^{\max}$ is a material parameter equal to the corresponding fracture energy density g_f, which is derived from the fracture mechanics as $g_f^d = G_f^d/l_c$, where G_f^d the tensile fracture energy and l_c is the characteristic length of the fractured domain employed in the regularization process. An identical procedure gives the fracture energy density g_c^d for a compression process yielding to the following expressions for $\kappa = 1/[(\Xi_c^{\max}\rho_0 E^0)/f_c^2 - 1/2] \geq 0$. Due to the fact that the value of κ have to be the same for a compression or tension test, we have that $\Xi_c^{\max} = \Xi_t^{\max} n^2$.

Tangent constitutive tensor. Starting from Eq. (10) and after several algebraic manipulations which can be reviewed in [1, 6], we obtain that the material form of the *tangent constitutive* tensor $\boldsymbol{\mathcal{C}}^{\mathrm{mt}}$ can be calculated as

$$\delta\hat{P}_1^{\mathrm{m}} = \boldsymbol{\mathcal{C}}^{\mathrm{mt}}\delta\hat{\mathcal{E}}_n = \big[(1-d)\mathbf{I} - \frac{\mathrm{d}G}{\mathrm{d}\mathcal{P}}\hat{P}_{01}^{\mathrm{m}} \otimes \frac{\partial \mathcal{P}}{\partial \hat{P}_{01}^{\mathrm{m}}}\big]\boldsymbol{\mathcal{C}}^{\mathrm{me}}\delta\hat{\mathcal{E}}_n \tag{21}$$

where $\mathbf{I}$ is the identity tensor. It is worth noting that $\boldsymbol{\mathcal{C}}^{\mathrm{mt}}$ is nonsymmetric and it depends on the elastic FPK stress vector.

3.1.2 Plastic materials

The model here presented is adequate to simulate the mechanical behavior of metallic and ceramic materials [16]. Assuming a thermally stable process and small elastic and finite plastic deformations, we have that the free energy density, Ψ, is given by the addition of the elastic and the plastic parts as

$$\Psi = \Psi^e + \Psi^P = \frac{1}{2\rho_0}(\hat{\mathcal{E}}_n^e \cdot \boldsymbol{\mathcal{C}}^{\mathrm{me}}\hat{\mathcal{E}}_n^e) + \Psi^P(k_p) \tag{22}$$

where the $\hat{\mathcal{E}}_n^e$ is the elastic strain calculated subtracting the plastic strain $\hat{\mathcal{E}}_n^P$ from $\hat{\mathcal{E}}_n$, Ψ^e and Ψ^P are the elastic and plastic parts of the free energy density, respectively, ρ_0 is the density in the material configuration and k_p is the *plastic damage* internal variable.

Constitutive equation. Employing the CP inequality and the Coleman's principle [10, 13], the secant constitutive equation and the mechanical dissipation take the following forms

$$\hat{P}_1^{\mathrm{m}} = \rho_0 \frac{\partial \Psi(\hat{\mathcal{E}}_n^e, k_p)}{\partial \hat{\mathcal{E}}_n^e} = \boldsymbol{\mathcal{C}}^{\mathrm{ms}}\big(\hat{\mathcal{E}}_n - \hat{\mathcal{E}}_n^P\big) = \boldsymbol{\mathcal{C}}^{\mathrm{me}}\hat{\mathcal{E}}_n^e \tag{23a}$$

$$\dot{\Xi}_m = \frac{\hat{P}_1^{\mathrm{m}} \cdot \dot{\hat{\mathcal{E}}}_n^P}{\rho_0} - \frac{\partial \Psi^P}{\partial k_p}\dot{k}_p \geq 0 \tag{23b}$$

where the material description of the secant constitutive tensor $\boldsymbol{\mathcal{C}}^{\text{ms}}$ coincides with $\boldsymbol{\mathcal{C}}^{\text{me}} = \text{Diag}[E_0, G_0, G_0]$.

Yield and plastic potential functions. Both, the yield function, $\mathcal{F}_p$, and plastic potential function, $\mathcal{G}_p$, are formulated in terms of the material form of the FPK stress vector $\hat{P}_1^{\text{m}}$ and the plastic damage internal variable k_p as

$$\mathcal{F}_p(\hat{P}_1^{\text{m}}, k_p) = \mathcal{P}_p(\hat{P}_1^{\text{m}}) - f_p(\hat{P}_1^{\text{m}}, k_p) = 0; \qquad \mathcal{G}_p(\hat{P}_1^{\text{m}}, k_p) = \mathcal{K} \tag{24}$$

where $\mathcal{P}_p(\hat{P}_1^{\text{m}})$ is the (scalar) equivalent stress, which is compared with the *hardening* function $f_p(\hat{P}_1^{\text{m}}, k_p)$ depending on the damage plastic internal variable k_p and the current stress state, and $\mathcal{K}$ is a constant value [16].

According to the evolution of the plastic damage variable, k_p, it is possible to treat materials considering *isotropic* hardening as in references [5, 18, 26]. However, in this work k_p constitutes a measure of the energy dissipated during the plastic process and, therefore, it is well suited for materials with *softening*. In this case k_p is defined [17] as

$$g_f^P = \frac{G_f^P}{l_c} = \int_{t=0}^{\infty} \hat{P}_1^{\text{m}} \cdot \dot{\mathcal{E}}_n^P \text{d}t; \qquad 0 \leq \big[k_p = \frac{1}{g_f^P} \int_{t=0}^{t} \hat{P}_1^{\text{m}} \cdot \dot{\mathcal{E}}_n^P dt\big] \leq 1 \tag{25}$$

where G_f^P is the specific plastic fracture energy of the material in tension and l_c is the length of the fractured domain defined in analogous manner as for the damage model. The integral term in Eq. (25) corresponds to the energy dissipated by means of plastic work and, therefore, k_p constitutes a measure of the part of the fracture energy that has been consumed during the deformation. Similarly, it is possible to define the normalized plastic damage variable for the case of a compressive test related with g_c^P.

Evolution laws for the internal variables. The flow rules for the internal variables $\hat{\mathcal{E}}_n^P$ and k_p are defined [11] according to

$$\dot{\hat{\mathcal{E}}}_n^P = \dot{\lambda} \frac{\partial \mathcal{G}_p}{\partial \hat{P}_1^{\text{m}}}; \qquad \dot{k}_p = \dot{\lambda}\, \hat{\varrho}(\hat{P}_1^{\text{m}}, k_p, G_f^P) \cdot \frac{\partial \mathcal{G}_p}{\partial \hat{P}_1^{\text{m}}} = \hat{\varrho}(\hat{P}_1^{\text{m}}, k_p, G_f^P) \cdot \dot{\hat{\mathcal{E}}}_n^P \tag{26}$$

where $\dot{\lambda}$ is the plastic consistency parameter and $\hat{\varrho}$ [16] is

$$\dot{k}_p = \big[\frac{r}{g_f^P} + \frac{1-r}{g_c^P}\big] \hat{P}_1^{\text{m}} \cdot \dot{\hat{\mathcal{E}}}_n^P = \widehat{\varrho} \cdot \dot{\hat{\mathcal{E}}}_n^P \tag{27}$$

The term $\hat{P}_1^{\text{m}} \cdot \dot{\hat{\mathcal{E}}}_n^P$ is the plastic dissipation and r is given in Eq. (12b). It is interesting to note that the proposed evolution rule distributes the total plastic dissipation as weighted parts of the compressive and tensile fracture energy densities. In what regards the hardening function of Eq. (24), the following evolution equation has been proposed:

$$f_p(\hat{P}_1^{\text{m}}, k_p) = r\sigma_t(k_p) + (1-r)\sigma_c(k_p) \tag{28}$$

where r has been defined in Eq. (12b) and the functions $\sigma_t(k_p)$ and $\sigma_c(k_p)$ represent the evolution of the yielding threshold in uniaxial tension and compression tests, respectively.

As it is a standard practice in plasticity, the loading/unloading conditions are derived in the standard form from the Kuhn-Tucker relations formulated for problems with unilateral restrictions,

i.e. , (a) $\dot{\lambda} \geq 0$, (b) $\mathcal{F}_p \leq 0$ and (c) $\dot{\lambda}\mathcal{F}_p = 0$. Starting from the plastic consistency condition $\dot{\mathcal{F}}_p = 0$, and considering the flow rules of Eqs. (26), we have that $\dot{\lambda}$ is

$$\dot{\lambda} = -\frac{\frac{\partial \mathcal{F}_p}{\partial \hat{P}_1^{\mathrm{m}}} \cdot (\boldsymbol{\mathcal{C}}^{\mathrm{me}} \dot{\hat{\mathcal{E}}}_n)}{\left\{ \frac{\partial \mathcal{F}_p}{\partial \hat{P}_1^{\mathrm{m}}} \cdot (\boldsymbol{\mathcal{C}}^{\mathrm{me}} \frac{\partial \mathcal{G}_p}{\partial \hat{P}_1^{\mathrm{m}}}) - \frac{\partial f_p}{\partial k_p} \hat{\varrho} \cdot \frac{\partial \mathcal{G}_p}{\partial \hat{P}_1^{\mathrm{m}}} \right\}} \tag{29}$$

The material form of the tangent constitutive tensor is calculated taking the time derivative of Eq. (23a), considering Eq. (26) and replacing the plastic consistency parameter of Eq. (29), and after several algebraic manipulations, it is obtained as [16, 17]

$$\delta \hat{P}_1^{\mathrm{m}} = \Big[\boldsymbol{\mathcal{C}}^{\mathrm{me}} - \frac{\big(\boldsymbol{\mathcal{C}}^{\mathrm{me}} \frac{\partial \mathcal{G}_p}{\partial \hat{P}_1^{\mathrm{m}}}\big) \otimes \big(\boldsymbol{\mathcal{C}}^{\mathrm{me}} \frac{\partial \mathcal{F}_p}{\partial \hat{P}_1^{\mathrm{m}}}\big)}{\frac{\partial \mathcal{F}_p}{\partial \hat{P}_1^{\mathrm{m}}} \cdot \big(\boldsymbol{\mathcal{C}}^{\mathrm{me}} \frac{\partial \mathcal{G}_p}{\partial \hat{P}_1^{\mathrm{m}}}\big) - \frac{\partial \mathcal{F}_p}{\partial k_p} \hat{\varrho} \cdot \big(\frac{\partial \mathcal{G}_p}{\partial \hat{P}_1^{\mathrm{m}}}\big)} \Big] \delta \hat{\mathcal{E}}_n = \boldsymbol{\mathcal{C}}^{\mathrm{mt}} \delta \hat{\mathcal{E}}_n \tag{30}$$

3.2 Mixing theory for composites

Each material point on the cross section is treated as a composite material according to the *mixing theory* [3, 16] considering the following assumptions: (i) Each composite has a finite number of components. (ii) Each component participates in the mechanical behavior according to its volumetric participation. (iii) All the components are subjected to the same strain field. The assumption (iii) implies that we have the following closing equation:

$$\hat{\mathcal{E}}_n \equiv (\hat{\mathcal{E}}_n)_1 = \cdots = (\hat{\mathcal{E}}_n)_q = \cdots = (\hat{\mathcal{E}}_n)_N \tag{31}$$

which imposes the strain compatibility between components. The free energy density of the composite, $\bar{\Psi}$, is written for the adiabatic case as

$$\bar{\Psi}(\hat{\mathcal{E}}_n, \alpha_p) \equiv \sum_{q=1}^{N} k_q \Psi_q(\hat{\mathcal{E}}_n, \alpha_p) \tag{32}$$

where $\Psi_q(\hat{\mathcal{E}}_n, \alpha_p)$ $(q = 1 \ldots N)$ is the free energy density of the q^{th} compounding substance which depends on p internal variables, $(\alpha_p)_q$, and $k_q = V_q/V$, the quotient between the volume of the q^{th} component, V_q, and the total volume, V, is the volumetric fraction of the component and, therefore, $\sum_q k_q = 1$ [3].
Starting from Eq. (32) and after applying the CP inequality and the Coleman's principle [10, 13], it is possible to obtain the material form of the FPK stress vector $\hat{P}_1^{\mathrm{m}}$ and the mechanical dissipation $\dot{\bar{\Xi}}_m$ for the composite in analogous way as for compounding substances, *i.e.*

$$\hat{P}_1^{\mathrm{m}} \equiv \bar{\rho}_0 \frac{\partial \bar{\Psi}(\hat{\mathcal{E}}_n, \alpha_p)}{\partial \hat{\mathcal{E}}_n} = \sum_{q=1}^{N} k_q (\rho_0)_q \frac{\partial \Psi_q(\hat{\mathcal{E}}_n, \alpha_p)}{\partial \hat{\mathcal{E}}_n} = \sum_{q}^{N} k_q (\hat{P}_1^{\mathrm{m}})_q \tag{33a}$$

$$\dot{\bar{\Xi}}_{\mathrm{m}} \equiv -\sum_{q=1}^{N} k_q (\dot{\Xi}_m)_q = -\sum_{q=1}^{N} k_q \Big[\sum_{m=1}^{p} \frac{\partial \Psi(\hat{\mathcal{E}}_n, \alpha_m)}{\partial \alpha_m} \dot{\alpha}_m \Big]_q \geq 0 \tag{33b}$$

where $\hat{P}_1^{\mathrm{m}}$ is obtained as a weighted sum, according to the volumetric fraction, of the material form of the stress vectors $(\hat{P}_1^m)_q$ corresponding to each one of the N components. In the same manner is obtained the total mechanical dissipation, $\dot{\bar{\Xi}}_m$, *i.e.* , considering the contribution of

the p internal variables of each one the compounding substances $(\dot{\Xi}_m)_q$.
The material form of the secant constitutive equation, the secant and tangent constitutive tensors, $\bar{\boldsymbol{\mathcal{C}}}^{\text{ms}}$ and $\bar{\boldsymbol{\mathcal{C}}}^{\text{mt}}$, for the composite are obtained as [16]

$$\bar{\boldsymbol{\mathcal{C}}}^{\text{ms}} \equiv \sum_{q=1}^{N} k_q(\boldsymbol{\mathcal{C}}^{\text{ms}})_q \rightarrow \hat{P}_1^{\text{m}} = \bar{\boldsymbol{\mathcal{C}}}^{\text{ms}}(\hat{\mathcal{E}}_n - \hat{\mathcal{E}}_n^P) \tag{34a}$$

$$\hat{\mathcal{E}}_n^P = \sum_{q=1}^{N} k_q(\hat{\mathcal{E}}_n^P)_q; \qquad \delta\hat{P}_1^{\text{m}} = \bar{\boldsymbol{\mathcal{C}}}^{\text{mt}}\delta\hat{\mathcal{E}}_n = \sum_{q=1}^{N} k_q(\boldsymbol{\mathcal{C}}^{\text{mt}})_q\delta\hat{\mathcal{E}}_n \tag{34b}$$

where $(\boldsymbol{\mathcal{C}}^{\text{ms}})_q$, $(\boldsymbol{\mathcal{C}}^{\text{mt}})_q$ and $(\hat{\mathcal{E}}_n^P)_q$ are the material form of the secant and tangent constitutive tensors and the material form of the plastic strain vector of the q^{th} component, respectively. The secant constitutive tensors of the right side of Eq. (34a) correspond to the elastic one if a plastic material is used and to these given in Eq. (10) if a damage model is used for the q^{th} component.

4 NUMERICAL IMPLEMENTATION

In order to obtain a Newton type numerical solution procedure, the linearized form of the weak form of Eq. (7) is required, which can be written as

$$\mathscr{L}[\mathrm{G}_{\text{w}}(\hat{\varphi}_*, \boldsymbol{\Lambda}_*, h)] = \mathrm{G}_{\text{w}}(\hat{\varphi}_*, \boldsymbol{\Lambda}_*, h) + D\mathrm{G}_{\text{w}}(\hat{\varphi}_*, \boldsymbol{\Lambda}_*, h)\cdot p \tag{35}$$

where $\mathscr{L}[\mathbf{G}_{\text{w}}(\hat{\varphi}_*, \boldsymbol{\Lambda}_*, h)]$ is the linear part of the functional $\mathrm{G}_{\text{w}}(\hat{\varphi}, \boldsymbol{\Lambda}, h)$ at the configuration defined by $(\hat{\varphi}, \boldsymbol{\Lambda}) = (\hat{\varphi}_*, \boldsymbol{\Lambda}_*)$ and $p \equiv (\Delta\hat{\varphi}, \Delta\hat{\theta}) \in \mathbb{R}^3 \times T_{\boldsymbol{\Lambda}}^{\text{spa}}$ is an admissible variation. The term $\mathrm{G}_{\text{w}}(\hat{\varphi}_*, \boldsymbol{\Lambda}_*, h)$ supplies the *unbalanced force* and the differential $D\mathrm{G}_{\text{w}}(\hat{\varphi}_*, \boldsymbol{\Lambda}_*, h)\cdot p$, the *tangential stiffness* [24] which is calculated as

$$\begin{aligned}
&D\mathrm{G}_{\text{w}}(\hat{\varphi}_*, \boldsymbol{\Lambda}_*, h)\cdot p = \\
&= \int_{[0,L]} \Big(\begin{bmatrix} \Delta\delta[\overset{\triangledown}{\hat{\gamma}}_{n*}] \\ \Delta\delta[\overset{\triangledown}{\hat{\omega}}_{n*}] \end{bmatrix}^T \begin{bmatrix} \hat{n}_* \\ \hat{m}_* \end{bmatrix} + \underbrace{\begin{bmatrix} \delta[\overset{\triangledown}{\hat{\gamma}}_{n*}] \\ \delta[\overset{\triangledown}{\hat{\omega}}_{n*}] \end{bmatrix}^T}_{([\mathbf{B}_*]h)^T} \begin{bmatrix} \Delta\hat{n}_* \\ \Delta\hat{m}_* \end{bmatrix} \Big) dS + \mathrm{K}_{\text{P}*} \\
&= \int_{[0,L]} \Big(h^T \underbrace{\begin{bmatrix} 0 & 0 \\ -\widetilde{\boldsymbol{n}}_*[\frac{\mathrm{d}}{\mathrm{d}S}] & 0 \end{bmatrix}}_{[\boldsymbol{n}_{S*}]} p + h^T[\mathbf{B}_*]^T \begin{bmatrix} \Delta\hat{n}_* \\ \Delta\hat{m}_* \end{bmatrix} \Big) dS + \mathrm{K}_{\text{P}*}
\end{aligned} \tag{36}$$

where the subscript $*$ has been written to indicate that the involved quantities have to be evaluated at $(\hat{\varphi}, \boldsymbol{\Lambda}) = (\hat{\varphi}_*, \boldsymbol{\Lambda}_*)$, the skew–symmetric tensor $\widetilde{\boldsymbol{n}}_*$ is obtained from its axial vector $\hat{n}_*$, the operator $[\frac{\mathrm{d}}{\mathrm{d}S}]$ is defined as $[\frac{\mathrm{d}}{\mathrm{d}S}]\hat{v} = [\mathbf{I}]\hat{v}_{,S}\ \forall\hat{v} \in \mathbb{R}^3$, the operator $[\boldsymbol{n}_{S*}]$ contributes to the geometric part of the tangent stiffness, the term $\mathrm{K}_{\text{P}*}$ corresponds to the part of the tangent stiffness which is dependent on the loading and the operator $[\mathbf{B}_*]$ relates the admissible variation h and the co–rotated variation of the reduced strain vectors. Explicit expressions for $\mathrm{K}_{\text{P}*}$ and $[\mathbf{B}_*]$ can be found in [9, 24].
The estimation of the linearized form of the sectional force and moment vectors appearing in Eq. (36) requires taking into account the linearized strain–stress relations existing between the

material form of the FPK stress vector $\hat{P}_1^m$ as follows

$$\Delta\hat{P}_1^{\mathrm{m}} = \bar{\boldsymbol{\mathcal{C}}}^{\mathrm{mt}}\Delta\hat{\mathcal{E}}_n = \boldsymbol{\Lambda}^T[\Delta\overset{\triangledown}{[\hat{P}_1]} - \widetilde{\boldsymbol{P}}_1\Delta\hat{\theta}] \tag{37a}$$

$$\Delta\overset{\triangledown}{[\hat{P}_1]} = \boldsymbol{\Lambda}\Delta\hat{P}_1^{\mathrm{m}} = (\boldsymbol{\Lambda}\bar{\boldsymbol{\mathcal{C}}}^{\mathrm{mt}}\boldsymbol{\Lambda}^T)\boldsymbol{\Lambda}\Delta\hat{\mathcal{E}}_n = \bar{\boldsymbol{\mathcal{C}}}^{\mathrm{st}}\Delta\overset{\triangledown}{[\hat{\varepsilon}_n]} \tag{37b}$$

$$= \boldsymbol{\Lambda}(\Delta(\boldsymbol{\Lambda}^T\hat{P}_1)) = \Delta\hat{P}_1 - \Delta\widetilde{\boldsymbol{\theta}}\hat{P}_1 \tag{37c}$$

where $\bar{\boldsymbol{\mathcal{C}}}^{\mathrm{mt}}$ is the material forms of the tangential constitutive tensors for the composite which are obtained from Eq. (34b) and the corresponding spatial form is obtained as $\bar{\boldsymbol{\mathcal{C}}}^{\mathrm{st}} = \boldsymbol{\Lambda}\bar{\boldsymbol{\mathcal{C}}}^{\mathrm{mt}}\boldsymbol{\Lambda}^T$. The skew-symmetric tensors $\Delta\widetilde{\boldsymbol{\theta}}$ and $\widetilde{\boldsymbol{P}}_1$ are obtained from the linear increment in the rotation vector $\Delta\hat{\theta}$ and the FPK stress vector $\hat{P}_1$, respectively.
Employing Eq. (37a) it is possible to obtain linearized constitutive relation between the material form of stress resultant and stress couple vectors and the reduced strain vectors as

$$\left\{\begin{array}{c}\Delta\hat{n}^{\mathrm{m}}\\ \Delta\hat{m}^{\mathrm{m}}\end{array}\right\} = \left[\begin{array}{cc}\mathbf{C}_{11}^{\mathrm{mt}} & \mathbf{C}_{12}^{\mathrm{mt}}\\ \mathbf{C}_{21}^{\mathrm{mt}} & \mathbf{C}_{22}^{\mathrm{mt}}\end{array}\right]\left\{\begin{array}{c}\Delta\hat{\Gamma}_n\\ \Delta\hat{\Omega}_n\end{array}\right\} \tag{38}$$

where $\mathbf{C}_{pq}^{\mathrm{mt}}$, $(p,q=1,2)$ are the material form of the *reduced tangential constitutive* tensors, which are calculated integrating over the beam cross section, as

$$\mathbf{C}_{11}^{\mathrm{mt}} = \int_{\mathcal{A}}\bar{\boldsymbol{\mathcal{C}}}^{\mathrm{mt}}d\mathcal{A}, \qquad \mathbf{C}_{12}^{\mathrm{mt}} = -\sum_{\beta=2}^{3}\int_{\mathcal{A}}\xi_\beta\bar{\boldsymbol{\mathcal{C}}}^{\mathrm{mt}}\widetilde{\boldsymbol{E}}_\beta d\mathcal{A} \tag{39a}$$

$$\mathbf{C}_{21}^{\mathrm{mt}} = \int_{\mathcal{A}}\widetilde{\boldsymbol{\Upsilon}}\bar{\boldsymbol{\mathcal{C}}}^{\mathrm{mt}}d\mathcal{A}, \qquad \mathbf{C}_{22}^{\mathrm{mt}} = -\sum_{\beta=2}^{3}\int_{\mathcal{A}}\xi_\beta\widetilde{\boldsymbol{\Upsilon}}\bar{\boldsymbol{\mathcal{C}}}^{\mathrm{mt}}\widetilde{\boldsymbol{E}}_\beta d\mathcal{A} \tag{39b}$$

where $\widetilde{\boldsymbol{\Upsilon}}$ and $\widetilde{\boldsymbol{E}}_\beta$ are the skew–symmetric tensors obtained from the vectors $\hat{\Upsilon} = \boldsymbol{\Lambda}^T(\hat{x}-\hat{\varphi})$ and $\hat{E}_\beta$, respectively. The corresponding *spatial reduced tangential tensors* are obtained as $\mathbf{C}_{pq}^{\mathrm{st}} = \boldsymbol{\Lambda}\mathbf{C}_{pq}^{mt}\boldsymbol{\Lambda}^T$, which are configuration dependent. The spatial form of the linearized relation of Eq. (38) can be obtained considering Eq. (37b) as

$$\left\{\begin{array}{c}\Delta\hat{n}\\ \Delta\hat{m}\end{array}\right\} = \underbrace{\left[\begin{array}{cc}\mathbf{C}_{11}^{\mathrm{st}} & \mathbf{C}_{12}^{\mathrm{st}}\\ \mathbf{C}_{21}^{\mathrm{st}} & \mathbf{C}_{22}^{\mathrm{st}}\end{array}\right]}_{[\mathbf{C}^{\mathrm{st}}]}\left\{\begin{array}{c}\Delta\overset{\triangledown}{[\hat{\gamma}_n]}\\ \Delta\overset{\triangledown}{[\hat{\omega}_n]}\end{array}\right\} - \underbrace{\left[\begin{array}{cc}0 & \widetilde{\boldsymbol{n}}\\ 0 & \widetilde{\boldsymbol{m}}\end{array}\right]}_{[\widetilde{\mathbf{F}}]}\left\{\begin{array}{c}\Delta\hat{\varphi}\\ \Delta\hat{\theta}\end{array}\right\} \tag{40}$$

where $\widetilde{\boldsymbol{m}}$ is the skew–symmetric tensor obtained from $\hat{m}$. Finally, Eq. (40) allows to rewrite Eq. (36) as

$$D\mathrm{G}_{\mathrm{w}*}\cdot p = \underbrace{\int_{[0,L]}h^T[\mathbf{B}_*]^T[\mathbf{C}_*^{\mathrm{st}}][\mathbf{B}_*]p\,dS}_{\mathrm{K}_{\mathrm{M}*}} + \underbrace{\int_{[0,L]}h^T([\widetilde{\boldsymbol{n}}_{S*}] - [\mathbf{B}_*]^T[\widetilde{\mathbf{F}}_*])p\,dS}_{\mathrm{K}_{\mathrm{G}*}} + \mathrm{K}_{\mathrm{P}*} \tag{41}$$

which allows to rewrite Eq. (35) as

$$\mathscr{L}[\mathrm{G}_{\mathrm{w}}(\hat{\varphi}_*,\boldsymbol{\Lambda}_*,h)] = \mathrm{G}_{\mathrm{w}}(\hat{\varphi}_*,\boldsymbol{\Lambda}_*,h) + \mathrm{K}_{\mathrm{M}*} + \mathrm{K}_{\mathrm{G}*} + \mathrm{K}_{\mathrm{P}*} \tag{42}$$

where $\mathrm{K}_{\mathrm{G}*}$ and K_{M*}, evaluated at the configuration $(\hat{\varphi}_*,\boldsymbol{\Lambda}_*)$, give the *geometric* and *material* parts of the tangent stiffness, which considers the inelastic behavior of the composite materials of the beam. The solution of the discrete form of Eq. (42) by using the FE method follows identical procedures as those described in [24] for an iterative Newton-Raphson integration scheme and it will not be repeated here.

4.1 Cross sectional analysis

The cross section analysis is carried out expanding each integration point on the beam axis in a set of integration points located on each fiber on cross section. Therefore, the beam cross section is meshed into a grid of quadrilaterals, each of them corresponding to a fiber oriented along the beam axis (see Figure 3). The estimation of the average stress on each quadrilateral is carried out by integrating the constitutive equations of the compounding materials of the composite associated to the quadrilateral and applying the mixing rule. The geometry of each quadrilateral is described by means of normalized bi-dimensional shapes functions and several integration points can be specified according to a selected integration rule. In the case of the average value of the material form of the FPK stress vector acting on a quadrilateral we have

$$\hat{P}_1^{\mathrm{m}} = \frac{1}{A_c}\int \hat{P}_1^{\mathrm{m}} dA_c = \frac{1}{A_c}\sum_{p=1}^{Np}\sum_{q=1}^{Nq} \hat{P}_1^{\mathrm{m}}(y_p, z_q) J_{pq} W_{pq} \tag{43}$$

where A_c is the area of the quadrilateral, Np and Nq are the number of integration points in the directions of the normalized geometry of the quadrilateral, $\hat{P}_1^{\mathrm{m}}(y_p, z_q)$ is the value of the FPK stress vector existing on an integration point with local coordinates (y_p, z_q), J_{pq} is the Jacobian of the transformation between normalized coordinates and cross sectional coordinates and W_{pq} are the weighting factors. The coefficients of the tangent constitutive tensors can be estimated in an analogous manner as in Eq. (43) but replacing $\hat{P}_1^{\mathrm{m}}(y_p, z_q)$ by $\bar{\boldsymbol{\mathcal{C}}}^{\mathrm{mt}}(y_p, z_q)$. Finally, the cross sectional forces and moments are obtained as

$$\hat{n}^{\mathrm{m}} = \sum_{k=1}^{Nfiber} (A_c)_k (\hat{P}_1^{\mathrm{m}})_k, \quad \hat{m}^{\mathrm{m}} = \sum_{k=1}^{Nfiber} (A_c)_k \hat{\ell}_k \times (\hat{P}_1^{\mathrm{m}})_k \tag{44}$$

were $Nfiber$ is the number of fibers, $(A_c)_k$ is the area of the k quadrilateral, $(\hat{P}_1^{\mathrm{m}})_k$ is the average value of the FPK stress vector and $\hat{\ell}_k = (0, y_k, z_k)$ are the coordinates of the gravity center of the k^{th} quadrilateral. By applying the same procedure as in Eq. (44), we have that the material form of the reduced tangential tensors of Eqs. (39a) and (39b) are numerically estimated as

$$\mathbf{C}_{11}^{\mathrm{mt}} = \sum_{k=1}^{Nfiber} (A_c)_k (\bar{\boldsymbol{\mathcal{C}}}^{\mathrm{mt}})_k; \qquad \mathbf{C}_{12}^{\mathrm{mt}} = -\sum_{k=1}^{Nfiber} (A_c)_k (\bar{\boldsymbol{\mathcal{C}}}^{\mathrm{mt}})_k (y_k \widetilde{\boldsymbol{E}}_2 + z_k \widetilde{\boldsymbol{E}}_3) \tag{45a}$$

$$\mathbf{C}_{21}^{\mathrm{mt}} = \sum_{k=1}^{Nfiber} (A_c)_k \widetilde{\boldsymbol{\ell}}_k (\bar{\boldsymbol{\mathcal{C}}}^{\mathrm{mt}})_k; \qquad \mathbf{C}_{22}^{\mathrm{mt}} = -\sum_{k=1}^{Nfiber} (A_c)_k \widetilde{\boldsymbol{\ell}}_k (\bar{\boldsymbol{\mathcal{C}}}^{\mathrm{mt}})_k (y_k \widetilde{\boldsymbol{E}}_2 + z_k \widetilde{\boldsymbol{E}}_3) \tag{45b}$$

where $\widetilde{\boldsymbol{\ell}}_k$ is the skew symmetric tensor obtained from $\hat{\ell}_k$ and $(\bar{\boldsymbol{\mathcal{C}}}^{\mathrm{mt}})_k$ is the material form of the tangent constitutive tensor for the composite material of the k^{th} quadrilateral.

From the point of view of the numerical implementations in a given loading step and iteration, two additional integration loops are required. The first one is a loop over the quadrilaterals. In this loop, having obtained the material form of the reduced strain measures $\hat{\Gamma}_n$ and $\hat{\Omega}_n$, the strain measure $\hat{\mathcal{E}}_n$ is calculated for each integration point on a quadrilateral. The second loop runs over each simple material associated to the composite of the quadrilateral. In this case, the FPK stress vector, P_1^{m}, and the tangent constitutive relation, $\boldsymbol{\mathcal{C}}^{\mathrm{mt}}$, are calculated for each component according to their specific constitutive equations; the behavior of the composite is recovered with the help of the mixing theory, summarized in Eqs. (33a) to (33b). Finally,

the discrete version of the spatial form of the reduced forces and moments, $\hat{n} = \mathbf{\Lambda}\hat{m}^{\mathrm{m}}$ and $\hat{m} = \mathbf{\Lambda}\hat{m}^{\mathrm{m}}$, and sectional tangent stiffness tensor $\mathbf{C}^{\mathrm{st}}_{ij} = \mathbf{\Lambda}\mathbf{C}^{\mathrm{mt}}_{ij}\mathbf{\Lambda}^T$ $(i,j = 1,2)$ are calculated [9].

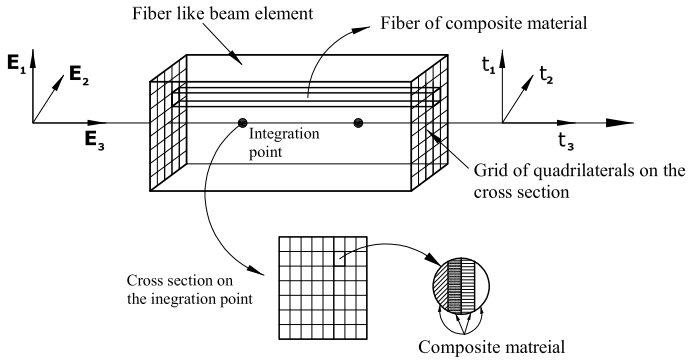

Figure 3: Discrete fiber like model of the beam element.

As it has been previously explained, the sectional behavior is obtained as the weighted sum of the contribution of the fibers. The nonlinear relation between the reduced strain measures and cross sectional forces and moments are obtained from Eq. (44).

5 DAMAGE INDEX

A measure of the damage level of a material point can be obtained as the ratio of the existing stress level, obtained applying the mixing rule, to its elastic counter part. Following this idea, it is possible to define the fictitious damage variable $\check{D}$ as follows

$$\sum_{i=1}^{3}|P^{\mathrm{m}}_{1i}| = (1-\check{D})\sum_{i=1}^{3}|P^{\mathrm{m}}_{1i0}| = (1-\check{D})\sum_{i=1}^{3}|(\boldsymbol{\mathcal{C}}^{\mathrm{m}}\hat{\mathcal{E}}_n)_i|; \qquad \check{D} = 1 - \frac{\sum_{i=1}^{3}|P^{\mathrm{m}}_{1i}|}{\sum_{i=1}^{3}|P^{\mathrm{m}}_{1i0}|} \tag{46}$$

where $|P^{\mathrm{m}}_{1i}|$ and $|P^{\mathrm{m}}_{1i0}|$ are the absolute values of the components of the existing and elastic stress vectors in material form, respectively. It is worth to note that $\check{D}$ considers any kind of stiffness degradation at the material point level through the mixing rule and then it constitutes a measure of the remaining load carrying capacity. Initially, the material remains elastic and $\check{D} = 0$, but when the entire fracture energy of the material has been dissipated $|P^{\mathrm{m}}_{1i}| \to 0$ and, therefore, $\check{D} \to 1$. Eq. (46) can be extended to consider elements or even the whole structure by means of integrating the stresses over a finite volume of the structure as $\check{D} = 1 - [\int_{V_p}\left(\sum_i |P^{\mathrm{m}}_{1i}|\right)\mathrm{d}V_p]/[\int_{V_p}\left(\sum_i |P^{\mathrm{m}}_{1i0}|\right)\mathrm{d}V_p]$, where V_p is the volume of the part of the structure.

6 NUMERICAL EXAMPLES

6.1 Mesh independent response of a composite cantilever beam

The RC cantilever beam shown in Figure 4 is used to study if, regularizing the dissipated energy at constitutive level, it is possible to obtain a mesh independent response.
Forty increments of imposed displacements were applied in the Y direction and four meshes of 10, 20 40 and 80 quadratic elements with the Gauss integration rule where considered in the simulations. The cross section was meshed into 20 equally spaced layers. The mechanical properties of the concrete and steel are summarized in Table 1, where E and ν are the elastic modulus and Poisson coefficient, respectively; G_f is the fracture energy, f_c is the ultimate

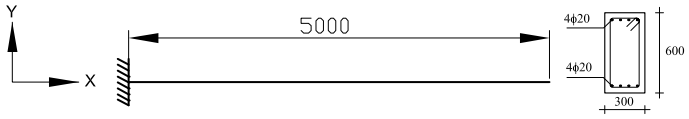

Figure 4: RC cantilever beam.

Table 1: Mechanical properties

	E Mpa	ν Mpa	f_c Mpa	n	G_f Nmm^{-2}
Concrete	21000	0.20	25	8	1
Steel	200000	0.15	500	1	500

compression limit and n is the ratio of the compression to the tension yielding limits.
Figure 5 shows the capacity curve relating the vertical reaction with the displacement of the free end. It is possible to see that the numerical responses converge to that corresponding to the model with the greater number of elements.

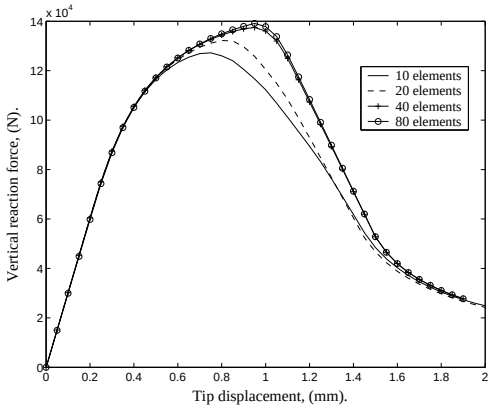

Figure 5: Vertical reaction versus tip displacement.

Further information can be obtained from the evolution of the local damage index at cross sectional level, which is shown in Figure 6 for the 4 meshes and the loading steps 10, 25 and 40. In all the cases, strain localization occurs in the first element but, in the case of the mesh with 10 elements, localization occurs before than in the other cases and a worse redistribution of the damage is obtained, what can explain the differences observed in Figure 5.

6.2 Framed dome

The elastic and plastic mechanical behavior of framed domes has been studied in several works [18, 27]. In this example, the nonlinear mechanical behavior of the framed dome shown in Figure 7 is studied with the objective of validating the proposed formulation in the inelastic range. The linear elastic properties of the material are: elastic modulus $20700\ MNm^{-2}$ and Poisson's coefficient 0.17. Three constitutive relations are employed: (1) Linear elastic; (2) Perfect plasticity ($G_f = 1 \times 10^{10}\ Nm^{-2}$) with associated Von Mises yield criterion and an elastic limit of $f_c = 80\ Nm^{-2}$; and (3) Damage model with equal tensile and compression limits, $n = 1$, a fracture energy of $G_{f,c} = 50\ Nm^{-2}$ and the same elastic limit as in case (2).
Three elements with two Gauss integration points are used for each structural member. A verti-

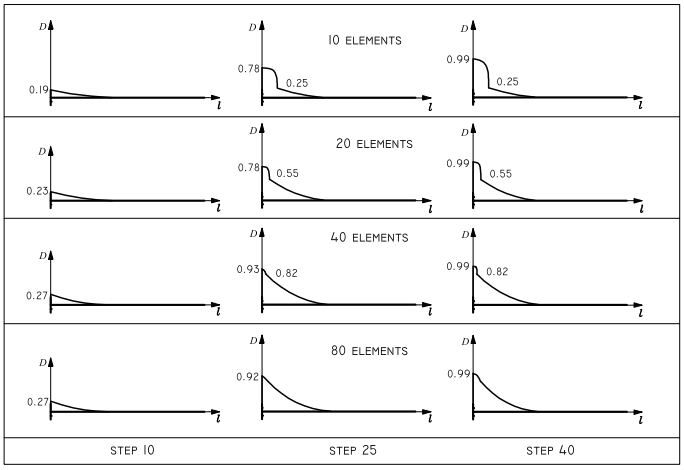

Figure 6: Evolution of the local cross sectional damage index: Strain localization. The symbols D and l are the damage index and the length of the beam, respectively.

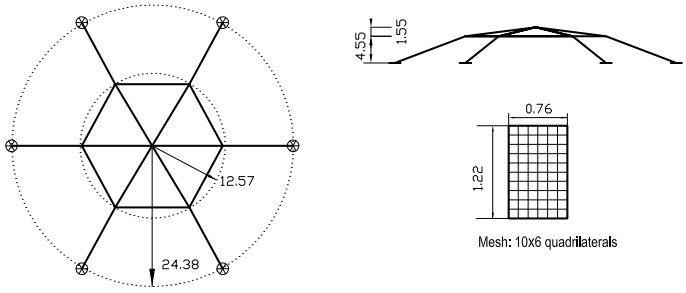

Figure 7: Framed dome and detail of the cross sectional mesh.

cal point load of $P_0 = 123.8\ N$ acting on the apex of the dome is applied and the displacement control technique is used in the simulations. Figure 8 shows the deflection of the vertical apex in function of the loading factor $\lambda = P_t/P_0$ (P_t is the current applied load) for the three constitutive relations. It is possible to see in Figure 8 a good agreement with the results given by Park and Lee in reference [18] for the stable branch of the elastic loading factor–displacement responses. When comparing both results for the elastic plastic case, it is possible to see a good agreement for the elastic limit of the structure; however, when deformation grows, the differences can reach 30% for the predicted value of the load carrying capacity of the dome. Moreover, the curve corresponding to the damage model has been added to Figure 8. In both cases, when inelastic constitutive relations are employed, the curve of the global structural response shows a snap–through which couples constitutive and geometric effects.

6.3 Nonlinear response of a forty–five degree cantilever bend

This example performs the coupled geometrically and constitutive nonlinear analysis of a cantilever bend placed in the horizontal X-Y plane, with a vertical load F applied at the free end, as shown in Figure 9. The radius of the bend has 100 mm with unitary cross section. This example has been considered in several works as a good validation test [7, 9, 24]. The mechanical properties for the elastic case are an elastic modulus of $1 \times 10^7\ Nmm^{-2}$ and a shear modulus of $5 \times 10^6\ Nmm^{-2}$. Four quadratic initially curved elements are used with two Gauss integration points per element. Solutions are obtained by using thirty equal load increments

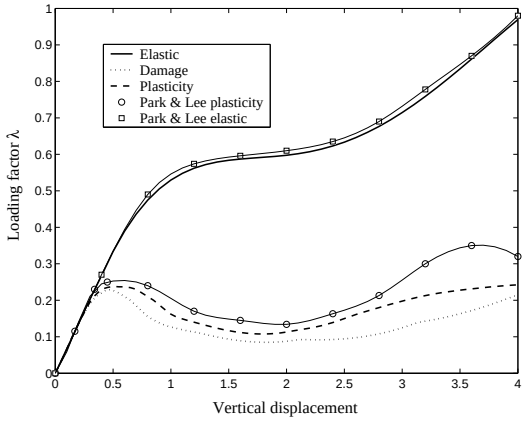

Figure 8: Loading factor-displacement curve of the vertical apex of the dome.

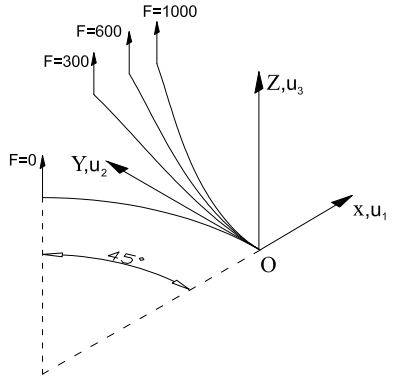

Figure 9: Initial geometry and some examples of the deformed configurations for the linear elastic case of the 45^0 cantilever bend.

of 100 N. The history of the tip displacements is shown in Figure 10. The tip displacements for an applied load of 600 N are: U_1=13.56 mm. U_2=-23.81 mm and U_3=53.51 mm (see Figure 9) which are values close to those obtained by other authors [9]. The coupled geometric

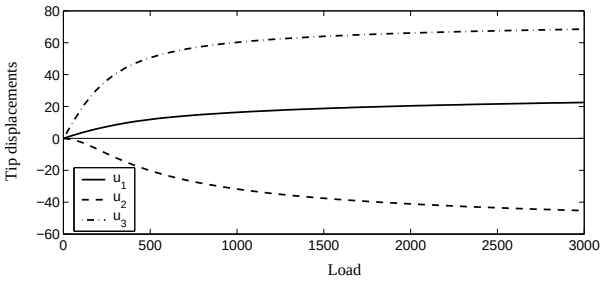

Figure 10: Different components of the tip displacement.

and constitutive nonlinear response was obtained for three materials: (i) Elastic–plastic with a fracture energy of $G_f = 1 \times 10^{10}\ Nmm^{-2}$, and a tension to compression ratio $n = 1$) (ii) Degrading material ($n = 1$, $G_f = 5 \times 10^4\ Nmm^{-2}$) and (iii) A composite formed by equal parts of the materials (i) and (ii). In all the cases, the elastic limit is taken $f_c = 7 \times 10^4\ Nmm^{-2}$. The beam cross section was meshed into a grid of 10×10 quadrilaterals and 35 imposed displacements of 2 mm was applied. The convergence tolerance was 10^{-4}. Figure 11

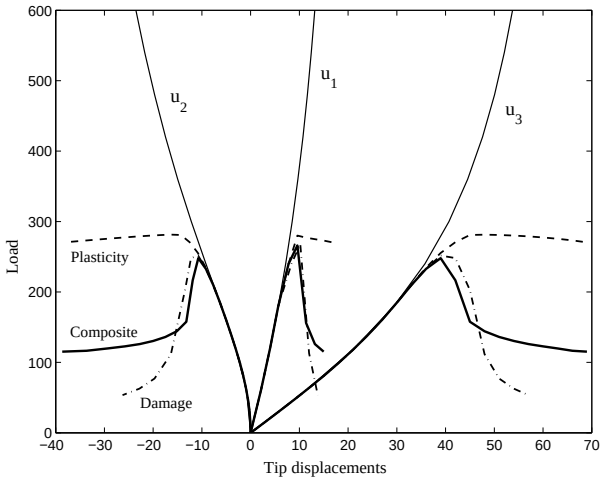

Figure 11: Different components of the tip displacement.

shows the results for the tip displacements superposed to the elastic response. It is possible to observe that: (1) The elastic plastic case converges to a fixed value of $274\ N$ for the vertical reaction after the redistribution of the damage has occurred, which can be considered the final stage in the formation of a plastic hinge. (2) In the case of the degrading material, the analyze were stopped in the loading step 29 due to lack of convergency with an evident loss in the load carrying capacity. (3) The response of the composite materials shows two phases: the first one corresponds to the degradation of the damaging phase; during the second one the vertical reaction is stabilized in a value equal to $112\ N$, due to the mechanical response of the plastic phase.

7 CONCLUSIONS

The Reissner–Simo geometrically exact formulation for 3D beams is considered in the context of initially curved beams and extended to include arbitrary distribution of composite materials in the cross sections. The resulting formulation is used for studying the constitutive and geometric nonlinear behavior of framed structures in the static case. Constitutive laws for the simple materials are based on thermodynamically consistent formulations. The simple mixing rule for composites is used for modeling complex material behaviors. A detailed cross sectional analysis, consistent with the kinematic hypothesis is presented. The proposed method, even when inexact from the point of view of the elasticity theory, gives a computationally convenient way of approximating the strain–stress distribution in the section. A mesh independent response is obtained by means of the regularization of the energy dissipated at constitutive level considering the characteristic length of the volume associated to a specific integration point and the fracture energy of the materials. Local and global damage indices have been developed based on the ratio between the elastic and nonlinear stresses. Several numerical examples have been included for the validation of the proposed formulation.

ACKNOWLEDGMENT

This research was partially supported by CEE–FP6 project FP6–505448 (GOCE), *Risk Mitigation for Earthquakes and Landslides* (LESSLOSS); by the Spanish Government: Ministerio de Fomento and Ministerio de Ciencia y Tecnología. Project Ref. MAT–2003–09768–C03–02, *Delamination of reinforced matrix composites* (DECOMAR); Ministerio de Educación y

Ciencia. Project BIA2005–06952, *Study of composite materials for design, reinforcement and retrofit of civil engineering structures* (RECOMP). The International Center for Numerical Methods in Enginnering (CIMNE) has also provided the support for this research. All this support is gratefully acknowledged.

REFERENCES

[1] A.H. Barbat, S. Oller, A. Hanganu, E. Oñate, Viscous damage model for Timoshenko beam structures, International Journal for Solids and Structures. 34 (1997) 3953–3976.

[2] A. Cardona, A. Huespe, Evaluation of simple bifurcation points and post-critical path in large finite rotations problems, Computer Methods in Applied Mechanics and Engineering. 175 (1999) 137–156.

[3] E. Car, S. Oller, E. Oñate, An anisotropic elasto plastic constitutive model for large strain analysis of fiber reinforced composite materials, Computer Methods in Applied Mechanics and Engineering. 185 (2000) 245–277.

[4] L. Davenne, F. Ragueneau, J. Mazars, A. Ibrahimbegović, Efficient approaches to finite element analysis in earthquake engineering, Computers and Structures. 81 (2003) 1223–1239.

[5] F. Gruttmann, R. Sauer and W. Wagner, Theory and numerics of three–dimensional beams with elastoplastic material behavior, International Journal of Numerical Methods in Engineering. 48 (2000) 1675–1702.

[6] A.D. Hanganu, E. Oñate, A.H. Barbat, Finite element methodology for local/global damage evaluation in civil engineering structures, Computers and Structures. 80 (2002) 1667–1687.

[7] A. Ibrahimbegović, On finite element implementation of geometrically nonlinear Reissner`s beam theory: three-dimensional curved beam elements, Computer Methods in Applied Mechanics and Engineering. 122 (1995) 11–26.

[8] A. Ibrahimbegović, M. Al Mikdad, Quadratically convergent direct calculation of critical points for 3D structures undergoing finite rotations, Computer Methods in Applied Mechanics and Engineering. 189 (2000) 107–120.

[9] R.K. Kapania, J. Li, On a geometrically exact curved/twisted beam theory under rigid cross–section assumption, Computational Mechanics. 30 (2003) 428–443.

[10] J. Lubliner, Thermomechanics of deformable bodies, Department of Civil Engineering, University of California, Berkeley, 1985.

[11] J. Lubliner, On the thermodynamic foundations of non–linear solid mechanics, International Journal of Non-Linear Mechanics. 7 (1972) 237-254.

[12] J. Mäkinen, H. Marjamäki, Total Lagrangian parametrization of rotation manifold, Fifth EUROMECH Nonlinear Dynamics Conference, Eindhoven, Netherlands. (2005) 522–530.

[13] L.E. Malvern, Introduction to the Mechanics of a Continuous Medium, Prentice–Hall, Englewood Cliffs, NJ, 1969.

[14] P. Mata A, S. Oller, A.H. Barbat, Static analysis of beam structures under nonlinear geometric and constitutive behavior, Computer Methods in Applied Mechanic and Engineering. (2007) (Accepted).

[15] P. Mata A, S. Oller, A.H. Barbat, Dynamic analysis of beam structures considering geometric and constitutive nonlinearity, Computer Methods in Applied Mechanic and Engineering. (2007) (Submitted).

[16] S. Oller, E. Oñate, J. Miquel, S. Botello, A plastic damage constitutive model for composites materials, International Journal of Solids and Structures. 33 (1996) 2501–2518.

[17] S. Oller, E. Oñate, J. Miquel, Mixing anisotropic formulation for the analysis of composites, Communications in Numerical Methods in Engineering. 12 (1996) 471–482.

[18] M.S. Park, B.C. Lee, Geometrically non–linear and elastoplastic three–dimensional shear flexible beam element of Von–Mises–type hardening material, International Journal for Numerical Methods in Engineering. 39 (1996) 383–408.

[19] P.K.V.V. Nukala, D.W. White, A mixed finite element for three–dimensional nonlinear analysis of steel frames, Computer Methods in Applied Mechanics and Engineering. 193 (2004) 2507–2545.

[20] E. Reissner, On one–dimensional large–displacement finite–strain beam theory, Studies in Applied Mathematics. 11 (1973) 87–95.

[21] M. Saje, G. Turk, A. Kalagasidu, B. Vratanar, A kinematically exact finite element formulation of elastic–plastic curved beams, Computers and Structures. 67 (1998) 197–214.

[22] G. Shi, S.N. Atluri, Elasto–plastic large deformation analysis of space–frames: a plastic hinge and stress–based explicit derivation of tangent stiffness, International Journal of Numerical Methods in Engineering. 26 (1988) 589–615.

[23] J.C. Simo, A finite strain beam formulation. The three-dimensional dynamic problem. Part I, Computer Methods in Applied Mechanics and Engineering. 49 (1985) 55–70.

[24] J.C. Simo, L. Vu-Quoc, A three-dimensional finite-strain rod model. Part II: Computational aspects, Computer Methods in Applied Mechanics and Engineering. 58 (1986) 79–116.

[25] J.C. Simo, L. Vu-Quoc, On the dynamics in space of rods undergoing large motions - A geometrically exact approach, Computer Methods in Applied Mechanics and Engineering. 66 (1988) 125–161.

[26] J.C. Simo, K.D. Hjelmstad, R.L. Taylor, Numerical simulations of elasto–viscoplastic response of beams accounting for the effect of shear, Computer Methods in Applied Mechanics and Engineering. 42 (1984) 301–330.

[27] G. Turkalj, J. Brnic, J. Prpic-Orsic, ESA formulation for large displacement analysis of framed structures with elastic–plasticity, Computers and Structures. 82 (2004) 2001–2013.